Adv. Polar Upper Atmos. Res., 15, 103–116, 2001

Initial results of Syowa MF radar observations in Antarctica

Masaki Tsutsumi, Takehiko Aso and Masaki Ejiri

National Institute of Polar Research, Kaga 1-chome, Itabashi-ku, Tokyo 173-8515

Abstract: Observations of the neutral atmosphere from the mesosphere to the lower thermosphere were performed using the MF radar system that was installed at Syowa Station (69°S, 39°E), Antarctica in April 1999. The radar is equipped with four antennas and independent receivers and is able to conduct interferometric observations, such as meteor echo observations, in addition to observations based on conventional spaced antenna techniques. Observational parameters are carefully designed so that the same raw data can be processed using various analysis techniques, including correlation analyses, meteor echo analysis and electron density analysis. The radar equipment specifications and preliminary results of wind observations are presented.

1. Introduction

A comprehensive understanding of Earth's atmosphere requires global observations from low latitude regions up to and including the polar regions. However, research on the polar atmosphere has fallen behind, especially in the Antarctic region because of the poor accessibility of these areas. The National Institute of Polar Research (NIPR), Japan recently began to conduct observations of the Antarctic mesosphere and lower thermosphere at Syowa Station (69°S, 39°E) using various measurement techniques, including an MF radar, a sodium temperature lidar, a Fabry-Perot interferometer, and an all-sky imager (Ejiri *et al.*, 1999). In this paper the initial results of the Syowa MF radar (since April 1999) are presented.

The basic idea for the new MF radar project at Syowa Station was presented by Tsutsumi *et al.* (1997) prior to its installation. MF radars are a powerful tool for measuring winds in the mesosphere and lower thermosphere and have been used to obtain information on the dynamics in these regions (*e.g.*, Vincent, 1984). The radars are equipped with at least three receiving antennas and usually employ a spaced antenna technique, mostly a full correlation analysis (FCA) (Briggs, 1984). The technique is characterized by its high temporal and height resolutions (about 2 min–4 km at most), and is used to study a wide period range of atmospheric phenomena, from short period gravity waves to mean winds at an altitude of 60–100 km. Recently, the accuracy of spaced antenna measurements performed using MF radars in the lower thermosphere, usually above 90 km, has been discussed (*e.g.*, Cervera and Reid, 1995). Although further intensive study is necessary, the importance of spaced antenna measurements, at least in the mesosphere, remains unchanged. On the other hand, other wind measurement techniques utilizing a radio interferometer have been also proposed (*e.g.*, Vandepeer and Reid, 1995; Thorsen *et al.*, 1997). Tsutsumi *et al.* (1999) presented meteor

wind observations made using an MF radar and have shown that wind measurements can be performed above 100 km, up to at least 114 km, using this technique. The Syowa MF radar is the only system in the Antarctic that is equipped with four receiving antennas, as opposed to the conventional three antenna systems; consequently, both spaced antenna and interferometry techniques can be applied.

In the following sections, we will describe the radar system and the newly designed observational parameters that enable the versatility of this system to be fully utilized (Section 2). We will also present the initial results of FCA and meteor wind observations that have been obtained (Section 3) and offer some concluding remarks (Section 4).

2. Radar system and observational parameters

2.1. Syowa MF radar system

The Syowa MF radar system was produced by Atmospheric Radar Systems (ATRAD), Australia, and was installed on East Ongul Island (69°S, 39°E), located near the coast of Antarctica, by members of the 40th Japanese Antarctic Research Expedition (JARE). Construction work was started in late December 1998, and completed in late March 1999. Continuous operation began on April 1st, 1999.

The basic parameters of the radar system are shown in Table 1. It is a mono-static pulse Doppler radar with a peak transmitting power of 50 kW and maximum duty ratio of 0.4%. The operating frequency is 2.4 MHz with a 99% power bandwidth of 60 kHz. The major advantage of the radar is that it has four antennas with each antenna being able to independently transmit and receive radio waves. The system can also perform various interferometric observations. Figure 1 shows the antenna configuration of the radar. The antenna array consists of four crossed dipole antennas located at the corners and center of a slightly deformed equilateral triangle, each side of which is about 150 m long. An equilateral triangle is the most favorable array shape for avoiding biases in measured wind velocities (Holdsworth, 1999). The shape of the Syowa system is slightly deformed because some antenna poles were shifted by a few meters from their planned positions when the ground conditions were found to be unsuitable. The minimum antenna spacing, which is the distance between the apex and the center of

Table 1. Common parameters for the two sets of observation parameters.

Operational frequency	2.4 MHz
Peak power	50 kW
Pulse repetition frequency	80 Hz
Transmission	
antenna array	four crossed dipoles
beam direction	zenith
Reception	
receivers	four receivers each of which is connected to a single crossed dipole
duration of each record	102.4 s
sampling range resolution	2 km

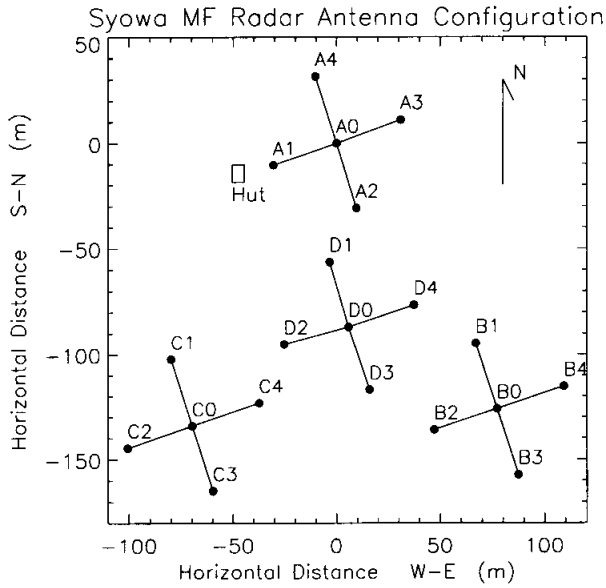

Fig. 1. Antenna configuration of Syowa MF radar. Each of the four crossed dipole antennas can be used for both transmission and reception.

the triangle, is 0.7λ. Most conventional MF radars are equipped with only three receiving antennas, and their spacing is longer than 1λ; thus, ambiguous echo arrival angles are unavoidable when the interferometric technique is applied.

Each dipole antenna is made of stainless wires (diameter, 4 mm) sustained at the center and both ends by aluminum poles (diameter, 7 cm). The tension of the wire can be adjusted using a winch fixed to each of the end poles. A balun box with a 1 : 1 transformer is placed at the top of each center pole. Low attenuation coaxial cables run from the baluns to the transmitters in the radar hut. To avoid impedance mis-matching between the antenna and the cable, all the electrical cable lengths are multiples of a half wavelength (2λ for all the antennas in the Syowa MF radar), so that impedance matching can be conducted by adjusting only one transformer at the final stage of the transmitter for each dipole antenna.

As all the crossed dipole antennas are excited in phase, all the antenna heights must be set at the same level to transmit the radio wave vertically. However, the radar is located in a hilly area, instead of a flat field. Thus, the lengths of the antenna poles vary from 1 m to 14 m, as required. The lengths are summarized in Table 2. Note that the antenna height from the ground can affect the antenna pattern. However, the Syowa MF radar is installed in a dry bedrock area, and the measured impedances of the eight dipole antennas are all close to 75 Ω throughout the year, regardless of the actual height of the pole from the ground. Thus, the electrical ground level can be considered to exist far below the actual ground surface. Consequently, the differences in the heights of the antennas from the solid ground to the top of the antenna do not have a significant effect on the radiation pattern.

Table 2. Lengths of antenna poles.

Antenna	A0	A1	A2	A3	A4	B0	B1	B2	B3	B4
Height (m)	1.0	6.0	4.9	3.7	2.8	11.2	12.0	11.1	8.8	13.1
Antenna	C0	C1	C2	C3	C4	D0	D1	D2	D3	D4
Height (m)	8.6	9.0	5.6	6.2	9.7	7.7	5.0	9.3	9.9	10.0

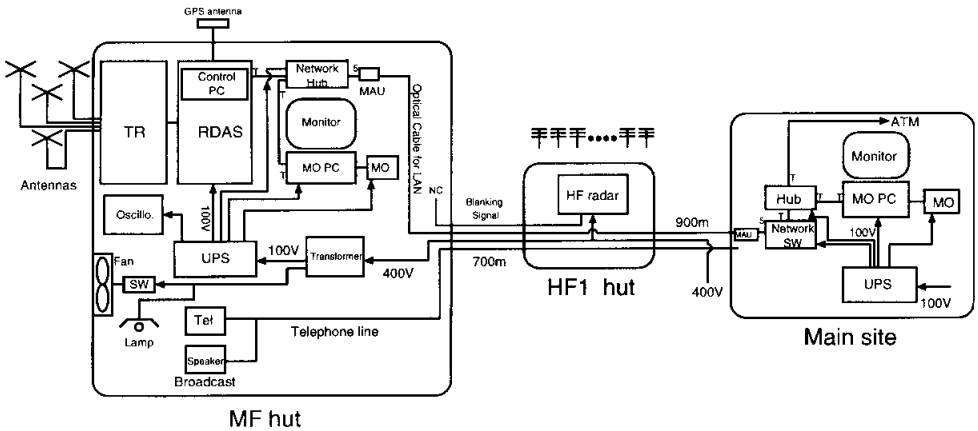

Fig. 2. Schematic diagram of the Syowa MF radar system. All of the equipment, other than the power supply, is in the radar hut located about 1 km away from the main site of the station.

The aluminum antenna poles are hinge-based and are supported with steel guy wires in four orthogonal directions. Each antenna base is directly fixed to the bedrock or a big rock with three anchor bolts. The poles can be raised up and down easily in case of antenna trouble.

Figure 2 shows a schematic diagram of the radar system. All the equipment, other than the power supply, are located in the radar hut. The hut is made of thick heat-insulated panels. The radar, especially the transmitter, generates enough heat to keep it running properly without the need for an additional heater, even during mid-winter when the outside temperature is as low as $-40°C$. In summer time, two electrical fans automatically ventilate the hut to release excessive heat and keep the room temperature below a preset level.

Electricity is supplied through a 1.6 km-long power cable that extends from the main site via one of the HF radar huts. Two other communications cables for telephone and LAN also run parallel to the power line. The radar can be controlled at the main site through the LAN connection.

The entire radar system in the MF radar hut is backed up by a 1.5 kVA UPS (Uninterruptive Power System). If the power supply is cut for some reason, a UPS-watching program detects the power failure and a series of procedures are automatically activated to safely shutdown the system. Thus, the entire operation of the MF radar is virtually automatic.

2.2. *Observational parameters*

The observational parameters are summarized in Tables 3 and 4. We have designed two special sets of parameters. The parameters are carefully chosen so that the acquired raw data can be processed using as many analysis techniques as possible. The two sets of parameters are alternated every two minutes.

Table 3. Observation Parameters 1.

Polarization	O mode
Coherent integration	16 times
Number of recorded data points	512
Sampling range	50–176 km

Table 4. Observation Parameters 2.

Polarization	O and X modes every 8 pulses
Coherent integration	8 times
Number of recorded data points	1024 (512 for each polarization)
Sampling range	50–138 km

The presence of the Earth's magnetic field produces differences in the propagation characteristics of the two polarization modes of radio waves; the ordinary (O) and the extraordinary (X) modes. The X mode is subject to a larger amount of absorption and group retardation in ionized atmosphere than the O mode; thus, the O mode is usually used for wind measurements obtained with MF radars. The differences in the propagation characteristics have been utilized to estimate electron density in the lower thermosphere (*e.g.*, Manson and Meek, 1984).

One of the two sets of parameters uses only the O mode, as shown in Table 3. Correlation techniques for wind measurements in the D region require a data length of about 2 min, a sampling frequency of about 2 Hz or higher, and a sampling range of 50–100 km (*e.g.*, Holdsworth and Reid, 1995). On the other hand, meteor echo observations require a faster sampling frequency and an extended sampling range to detect short-lived and long range echoes, respectively. After considering the size of the buffer memory and the data transfer speed, we selected an equivalent sampling frequency of 5 Hz after 16 coherent integrations and a sampling range of 50–176 km. The maximum observable Doppler frequency shift corresponding to the 5-Hz sampling frequency is 2.5 Hz. This further corresponds to the maximum observable radial wind velocity of $\lambda/2 \times 2.5 = 156$ m/s. This value is large enough for the present purpose because the largest possible horizontal wind velocity in the mesopause region is about 150 m/s and the observed radial velocity is the projection of the horizontal velocity to an off-zenith angle of about 30 degrees (where majority of echoes appear), that is, about 50% of the horizontal wind velocity. Raw data series acquired with this parameter set are processed using three different techniques: a full correlation analysis technique (FCA), a spatial correlation analysis technique (SCA), and a meteor echo analysis. The first two correlation techniques were coded by ATRAD; the meteor echo analysis software was

developed by the authors for Syowa MF radar based on the study by Tsutsumi *et al.* (1999).

The other set of observation parameters shown in Table 4 involves the transmission of both O and X mode radio waves alternatively every 0.1 s. The equivalent sampling frequency is 5 Hz for both modes, which is the same as the first set of observation parameters shown in Table 3. However, the maximum sampling range is reduced to 138 km from 176 km because of the buffer memory's limited size. Five analysis techniques are applied to the acquired data: a differential absorption experiment (DAE), a differential phase experiment (DPE), FCA, SCA, and the meteor echo analysis. Since the original correlation analysis suite by ATRAD was not designed to deal with raw data consisting of both polarizations, we modified the software so that each polarization data record can be extracted to reconstruct a new time series and used in the FCA, SCA and meteor echo analyses to produce both O and X mode winds independently. This modification to the analysis suite enables us to perform uninterrupted wind measurements even when the electron density measurements are conducted. The X mode wind velocities are actually by-products and not currently used for further analyses because the X mode is more severely absorbed and retarded than the O mode, as already described. Note, however, that the X mode wind measurements are thought to produce reasonable estimates in a low electron density environment. In the future, they will be combined with O mode wind data in an attempt to achieve better wind estimates.

The MF meteor echo analysis technique employed in the present study is basically the same as the one developed by Tsutsumi *et al.* (1999). We describe only one major improvement of the technique here. The real-time detection of meteor echoes is the most critical part of meteor echo observations. Tsutsumi *et al.* (1999) detected meteor echoes by searching time series of echo power that was produced by simply averaging the echo powers of all the receiver outputs. In the present study, we conducted a post-steering of the receiving antenna beam into several off-zenith directions. This technique significantly raises the SNR of meteor echoes. As a result, the number of detected echoes increased by roughly 50%

Acquired data is automatically transfered from the radar control PC (Personal Computer) in the radar hut to the monitor PC in the main site through a LAN (Local Area Network) and stored in an MO (Magneto Optical) disk. Since the bandwidth of the satellite data link between the Syowa Station and NIPR is rather narrow, the data is compressed into a very compact format of about 300 kB/day and transfered to NIPR, together with various diagnostic information regarding the radar system, on a daily basis.

3. Initial results

This section describes the first results of the FCA wind and meteor wind measurements.

3.1. FCA wind measurements

Figure 3 shows the 10-day mean acquisition rates for hourly FCA winds, where the

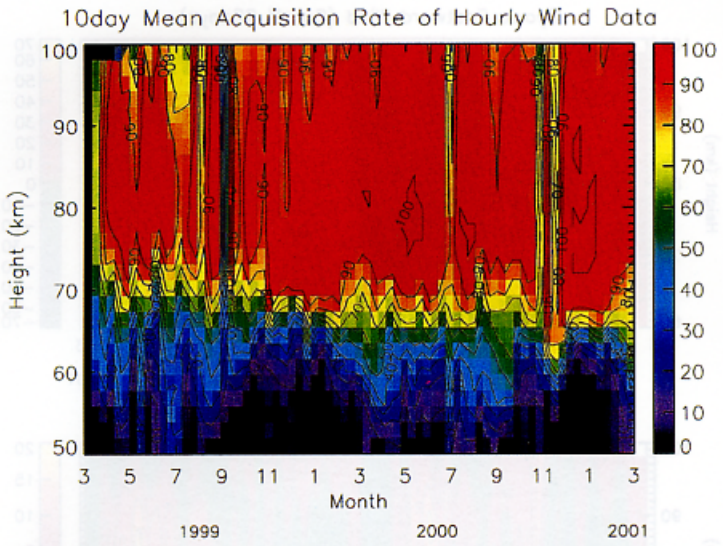

Fig. 3. Ten-day mean acquisition rate for hourly wind data obtained using O mode polarization. A value of 100 indicates that 24 data points were obtained in one day.

hourly winds are calculated only when more than three out of the 30 individual wind estimates an hour are successfully performed. Data acquisition rate is generally good throughout the year, especially above 70 km, where the rate is mostly greater than 90%. Even at 60 km, the rate is roughly 40–50%, except during the summer months. The two-year mean acquisition rate at 80 km was 94%. The rate for the year 2000 only was 96%. The quality of the data is high enough for various kinds of atmospheric waves to be studied. Wind velocities can quite often be estimated down to 50 km during the polar winter, when the ionization of the atmosphere by direct solar radiation is very weak. Other high-latitude MF studies have also reported similar phenomena (Igarashi 2001, private communications). Although the strong auroral activity in the polar region is thought to play an important role in ionization at lower altitudes, the precise mechanism of ionization is not well understood and remains an interesting topic that is worthy of future investigation.

The periods with low acquisition rates between July and September 1999 are mainly due to a hard disk crash that occurred on the radar control PC, a loose connection in one of the antenna balun boxes, and troubles with the power supply. Since these initial troubles, the radar system has been in continuous operation without any faults. The periods of low data acquisition seen in July 2000 and November 2000 correspond to events of severe radio wave absorption caused by high solar activities.

Figure 4 shows the prevailing winds at Syowa over two year observation period from April 1999 until March 2001. A low-pass filter with a cut off period of 20 days was applied. A very clear annual variation in the zonal component can be seen, flowing westward during the summer months and eastward during the other months. The peak westward velocity in summer is 40–50 m/s at around 78 km. In contrast, the peak eastward flow in winter is 20–40 m/s at 70 km or below and thus much weaker and

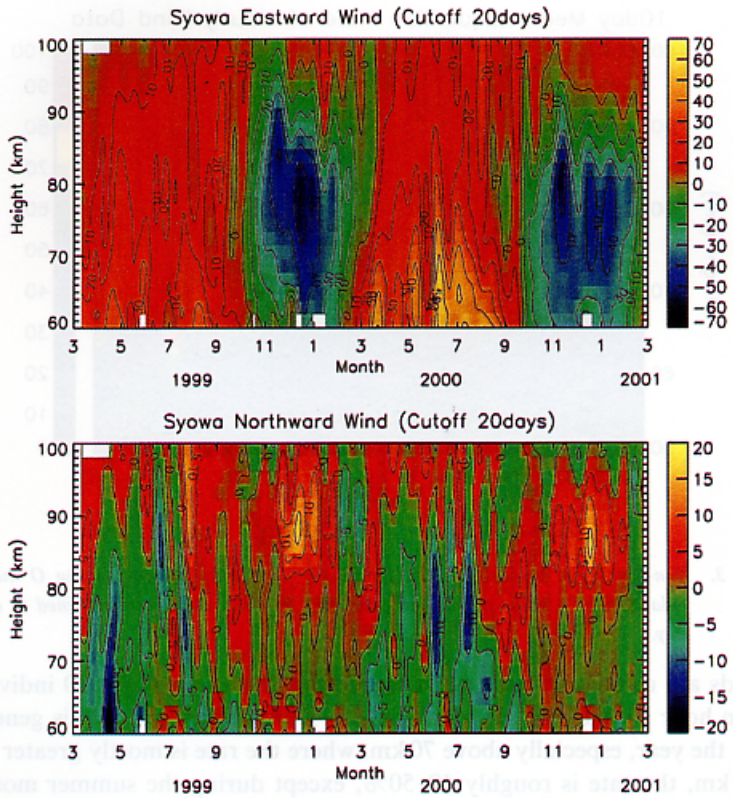

Fig. 4. Mean winds estimated using a full correlation analysis. The tick marks indicate the center of each month. A low-pass filter with a cut-off period of 20 days was applied.

located at a lower altitude than the summer peak. The most notable features are a strong vertical shear located above each summer-time peak and a reversal in wind direction between 90 and 100 km. The winter-time jets also become weaker at greater heights but do not reverse. These structures in the zonal component are associated with distinctive structures in the meridional component. Summer-time meridional winds generally flow northward (equatorward) with a peak of about 10 m/s at 88–90 km, which corresponds to the region of the strong vertical shear in the zonal component. The winter time meridional flow is a little more complicated. The flow fluctuates around zero or exhibits a slight northward movement above 90 km, but is southward (poleward) at lower altitudes. The southward flow peaks at about 10 m/s but has very limited period, again at the region of the strong vertical shear in the zonal component.

These phenomena seen in the mean wind analysis, especially the reversal in zonal flow in summer, have been studied by some authors from the view-point of wave-driven circulation (*e.g.*, Vincent, 1994; Fritts and Luo, 1995; Dowdy *et al.*, 2001). Summer-time meridional jets have also been reported for the Arctic region (*e.g.*, Manson and Meek, 1991). These structures are now believed to be maintained by dissipating and breaking atmospheric waves in this region. Vincent (1994) presented the results of MF

radar observations made at Mawson (67°S, 63°E), Antarctica from 1984 to 1990. Most of the characteristics reported by Vincent (1994) have been reproduced in the present study. One important progress made with the new observations is that the observable height range was expanded down to at least 60 km, thanks to the recent development of radar techniques. The study by Vincent (1994) is limited to the height region of 78–100 km and does not report the winter-time jet observed below 80 km and shown in Fig. 4. This jet suggests that wave driving is also important for the maintenance of the mean state in winter, although it may not be as crucial as it is in summer.

Another new feature identified by the present study is the existence of oscillatory structures with a period of around one month that are seen in both the zonal and meridional components. These structures are not seen in the plots by Vincent (1994), which are based on a 6-year average of wind fields. At the moment, the origin of these oscillatory structures is not known. Long-period traveling planetary waves and/or stationary waves may be possible sources. Luo *et al.* (2001) reported oscillations with a long period (20–40 day) in the mesopause region using several MF radar data obtained in the northern hemisphere, and discussed the possible relation between this phenomenon and the short-term solar rotation period (~27 days). The newly formed radar network in Antarctica may be able to provide a solution.

Figure 5 presents the frequency power spectrum of horizontal wind velocities calculated using observations over a two-year period from April 1999 to March 2001. First, the time series of hourly horizontal wind velocities at five heights from 80 to 88 km were separated into 40-day long segments. Then, the mean spectrum shown in the figure was obtained by averaging all the spectra for the individual segments. The most prominent wave is a semidiurnal tide with amplitudes in the zonal and meridional components that are comparable with each other. The second most prominent wave is a 24-hour tide, again with comparable amplitudes in the two components. Small but distinct peaks are also detected at higher frequency tidal components of 8, 6 and possibly 4 hours. Regions with periods of shorter than 12 hours exhibit a smooth logarithmic slope of about -2. Considering that the inertial period at Syowa is 12.9 hours, this region is mostly dominated by gravity waves, except for the high-frequency tidal components. The spectral density in regions with periods of longer than one day gradually increases with the period. No discernible clear peaks are seen in these regions. Since the spectra calculations are based on 40-day long segments, the oscillatory structure with the period of around one month shown in Fig. 4 can not be resolved in Fig. 5. Energy levels in the zonal and meridional components are almost the same in the range between 1 and 3 days, but those in the zonal component become larger for longer periods.

3.2. Meteor wind measurements

The distributions of 24680 underdense meteor echoes observed in June 1999 are shown in Fig. 6 as a function of height, local time and zenith angle. The entire month occurred during a polar night period, so the solar radiation did not reach the lower thermosphere. Figure 6a shows the height distribution, indicating that the echoes ranged from 80 km to 120 km. It is noteworthy that a large number of echoes were detected well above 100 km, where wind measurements are difficult to conduct using

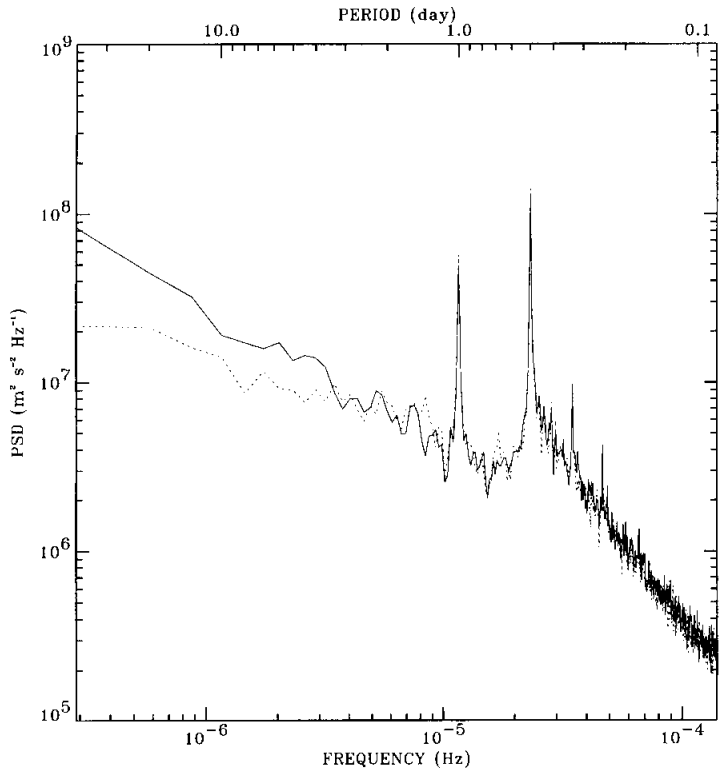

Fig. 5. Power spectrum density of hourly mean horizontal wind velocities estimated using two years of data obtained between April 1999 and March 2001. The spectra from 80 km to 88 km are averaged. Solid and dashed lines correspond to the zonal and meridional components, respectively.

correlation techniques. The mean value and standard deviation are 99.9 km and 6.8 km, respectively. These values are similar to those reported by Tsutsumi *et al.* (1999), which were based on observation performed on one night in October 1997 using the Buckland Park (35°S, 138°E) MF radar (1.98 MHz). The mean height of the present study, however, is about 5 km lower than that of the study by Tsutsumi *et al.* (1999). This difference is a result of the very limited observation period of Tsutsumi *et al.* (1999) and the differences in latitude, season, system setup, and observation parameters.

Figure 6b shows the local time dependence of the underdense echo rate in June 1999. The number of echoes detected on a given day is usually around 1000 but sometimes drops to as low as somewhere around 300. This reduction seems to be related to strong auroral activities that enhance the number density of electrons in the lower thermosphere and hinder the radio waves from penetrating the region. This is the major disadvantage of meteor observations made using an MF system. This situation does not occur when a VHF system is used because the radio frequency is usually sufficiently high compared with the plasma frequency in the region. Because of the effect of auroral activity on the echo rate, explaining the variation seen in Fig. 6b is not as simple as that for VHF radar measurements, in which a simple geometrical model

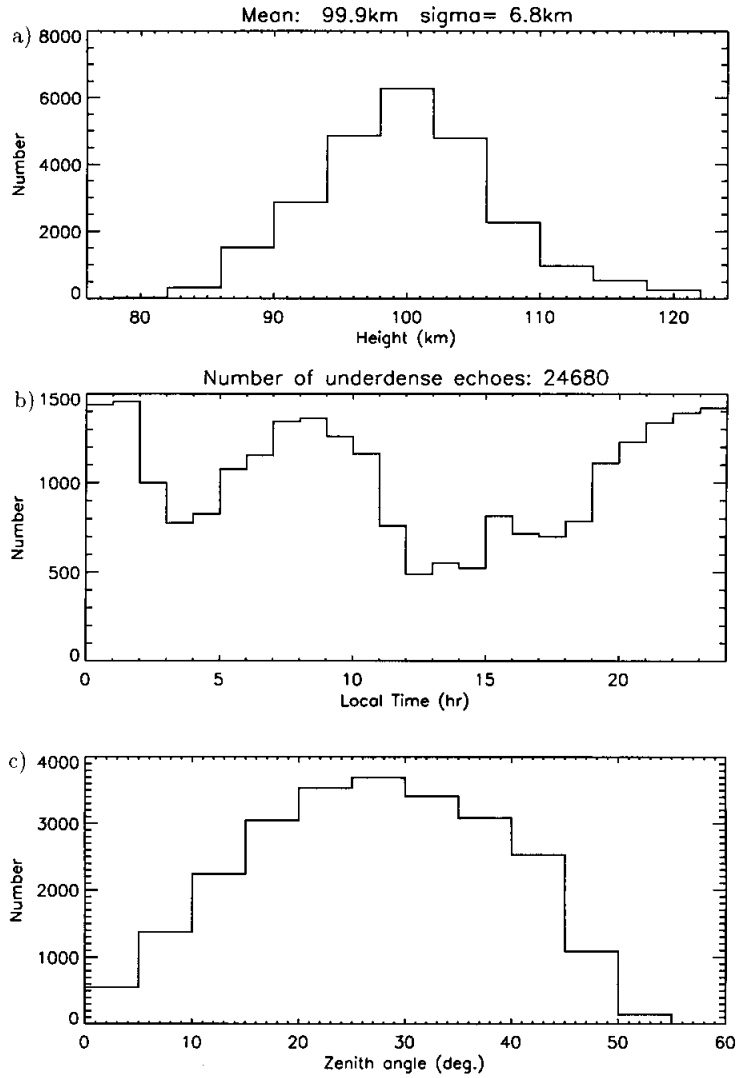

Fig. 6. Distribution of underdense meteor echoes obtained using O mode observations during June 1999. (a) Height distribution. (b) Hourly echo rates. (c) Zenith angle distribution.

can provide a good estimate of the local time dependence. Note, however, that wind data for all the local times can be obtained during the polar night period, enabling the study of atmospheric tides, planetary waves, and occasionally long period gravity waves. Wind velocities can be estimated with time and height resolutions of 2 hours and 4 km, respectively, when the auroral activity is not very high. The number of underdense echoes detected in June 2000 was 22020, which is slightly less than the results for June 1999. As the years 1999 and 2000 correspond to the periods of maximum solar activity, higher and more stable meteor echo rates can be expected for periods of lower solar

activity.

On the other hand, summer-time MF meteor observations are limited to only a few hours of weaker solar radiation around midnight, although the echo rates during these hours are comparable to those during winter or even higher. Echoes are sometimes detected during daylight hours, but these echoes often suffer severe group retardation. Hall (1998) estimated the difference between the true and virtual heights for a 2.8 MHz system in the auroral zone using model values. His results indicate that group retardation can be negligible around midnight in summer, but is significant around noon; total reflection can occur at altitudes as low as 90 km. The effect of group retardation must be corrected before summer-time meteor echo data can be applied to wind analyses.

Figure 6c displays the zenith angle distribution of underdense echoes. Almost all of the echoes are received from off-zenith angles, with a peak at around 25 degrees in spite of the fact that most of the radio wave energy is transmitted vertically. These results agree well with those of Tsutsumi *et al.* (1999), and indicate the importance of radio interferometry for determining the arrival angles of echoes.

Figure 7 exhibits an example of a time-height section of the horizontal winds. Horizontal wind vectors are estimated using a least-square method only when the number of underdense echoes in each time-height bin of 2 hours and 4 km exceeds five.

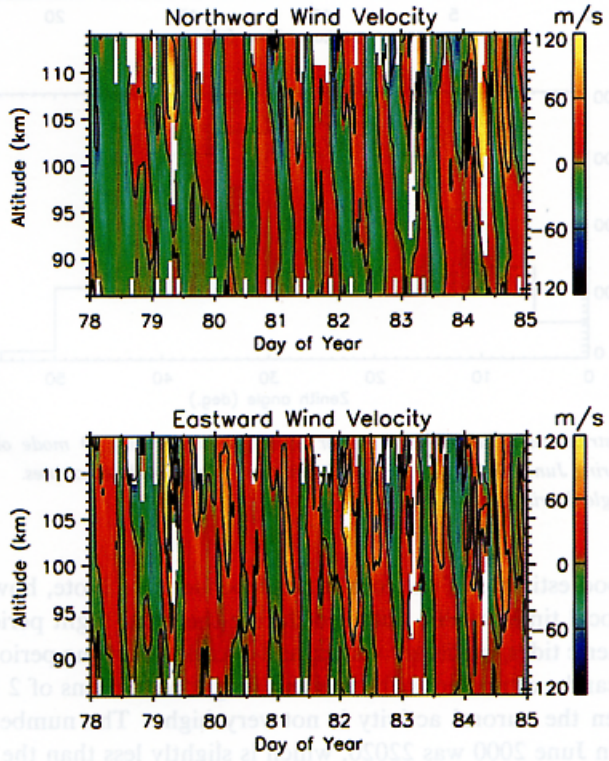

Fig. 7. Bihourly wind velocities for March 19–25, 2000, estimated using underdense meteor echoes.

No severe reduction in meteor echoes by auroral activity was seen during the observation period of March 19–25, 2000. The performance of the MF meteor observations is striking, showing a very clear semidiurnal tide in both the zonal and meridional components throughout the observed height range from 86 km to 114 km.

It is noteworthy that the lower part of the meteor wind observations overlaps with the upper part of the FCA observation. The MF meteor observations can, at least partly, compensate for potential problems in the FCA observation above 90 km, discussed in Section 1. On the other hand, the motion of meteor trails can also be affected by geomagnetic and electric fields, as described by Tsutsumi *et al.* (1999). A detailed comparison study between FCA winds and meteor winds is now being conducted.

4. Concluding remarks

We have built a new MF radar at Syowa Station (69°S, 39°E), in the Antarctica. The radar has been continuously operated without any major faults since April 1999. The most prominent feature of the radar is its ability to perform both spaced antenna and interferometric observations, using its four receiving antennas and receivers. Observational parameters can be selected to fully utilize the system's capabilities, and wind measurements using spaced antenna techniques (Full Correlation Analysis and Spatial Correlation Analysis) and an interferometric technique (meteor echoes) have been performed simultaneously. Preliminary results show that both FCA and meteor wind measurements can be successfully made. A study of comparing FCA wind and meteor wind measurements is now being performed; the results of the study will be reported elsewhere.

At Syowa Station, the use of various kinds of radio and optical instruments has also been recently initiated. These instruments include two HF SuperDARN radars, a sodium temperature lidar, a Fabry-Perot interferometer, and an all-sky airglow imager. These instruments, together with the MF radar, are expected to provide useful data on the vertical and horizontal structures of neutral winds and temperatures in the mesosphere and lower thermosphere. We are also looking forward to a collaborative study involving an MF radar network in the Antarctica (Davis (68.4°S, 77.6°E), Rothera (67.3°S, 68.1°W), Scott(77.5°S, 166.5°E) and Syowa) in the near future.

Acknowledgments

We are deeply grateful to those individuals who assisted with the installation of the Syowa MF radar.

The editor thanks to Drs. Y. Murayama and C. Hall for their help in evaluating this paper.

References

Briggs, B.H. (1984): The analysis of spaced sensor records by correlation techniques. Handbook for MAP, Vol 13. Urbana, SCOSTEP Secretariat, 166–186.

Cervera, M.A. and Reid, I.M. (1995): Comparison of simultaneous wind measurements using collocated VHF

meteor radar and MF space antenna radar systems. Radio Sci., **30**, 1245 1261.

Dowdy, A., Vincent, R.A., Igarashi, K., Murayama, Y. and Murphy, D.J. (2001): A comparison of mean winds and gravity wave activity in the northern and southern polar MLT. Geophys. Res. Lett., **28**, 1475-1478.

Ejiri, M., Aso, T., Okada, M., Tsutsumi, M., Taguchi, M., Sato, N. and Okano, S. (1999): Japanese research project on Arctic and Antarctic observations of the middle atmosphere. Adv. Space Res., **24**, 1689 1692.

Fritts, D.C. and Luo, Z. (1995): Dynamical and radiative forcing of the summer mesopause circulation and thermal structure 1. Mean solstice conditions. J. Geophys. Res., **100**, 3119-3128.

Hall, C. M. (1998): Virtual to true height correction for high latitude MF radar. Ann. Geophys., **16**, 277 279.

Holdsworth, D.A. (1999): Influence of instrumental effects upon the full correlation analysis. Radio Sci., **34**, 643-656.

Holdsworth, D.A. and Reid, I.M. (1995): A simple model of atmospheric radar backscatter: Description and application to the full correlation analysis of space antenna data. Radio Sci., **30**, 1263-1280.

Luo, Y., Manson, A.H., Meek, C.E., Igarashi, K. and Jacobi, Ch. (2001): Extra long period (20-40 day) oscillations in the mesospheric and lower thermosphere winds: observations in Canada, Europe and Japan, and considerations of possible solar influences. J. Atmos. Solar-Terr. Phys., **63**, 835-852.

Manson, A.H. and Meek, C.E. (1984): Partial reflection D-region electron densities. Handbook for MAP Vol 13. Urbana, SCOSTEP Secretariat, 113-123.

Manson, A.H. and Meek, C.E. (1991): Climatologies of mean winds and tides observed by medium frequency radars at Tromso (70°N) and Saskatoon (52°N) during 1987-1989. Can. J. Phys., **69**, 966 975.

Thorsen, D., Franke, S.J. and Kudeki, E. (1997): A new approach to MF radar interferometry for estimating mean winds and momentum flux. Radio Sci., **32**, 707-726.

Tsutsumi, M., Ejiri, M., Okano, S., Sato, N., Yamagishi, H., Igarashi, K. and Tsuda, T. (1997): MF radar observations of Antarctic mesosphere and lower thermosphere. Proc. NIPR Symp. Upper Atmos. Phys., **10**, 109-116.

Tsutsumi, M., Holdsworth, D., Nakamura, T. and Reid, I. (1999): Meteor observations with an MF radar. Earth Planets Space, **51**, 691-699.

Vandepeer, B.G.W. and Reid, I.M (1995): Some preliminary results obtained with the new Adelaide MF Doppler radar. Radio Sci., **30**, 1191-1203.

Vincent, R.A. (1984): MF/HF radar measurements of the dynamics of the mesopause region—A review. J. Atmos. Terr. Phys., **46**, 961-974.

Vincent, R.A. (1994): Gravity-wave motions in the mesosphere and lower thermosphere observed at Mawson, Antarctica. J. Atmos. Terr. Phys., **56**, 593-602.

(Received April 20, 2001; Revised manuscript accepted May 15, 2001)